Optical and electrical properties of amorphous zinc tin oxide thin films examined for thin film transistor application

Madambi K. Jayaraj[a)]
Optoelectronic Devices Laboratory, Department of Physics, Cochin University of Science and Technology, Kochi–682 022, India and Materials and Structures Laboratory, Mail Box R3-1, Tokyo Institute of Technology, 4259 Nagatsuta, Midori-ku, Yokohama, 226-8503, Japan

Kachirayil J. Saji
Optoelectronic Devices Laboratory, Department of Physics, Cochin University of Science and Technology, Kochi–682 022, India

Kenji Nomura, Toshio Kamiya, and Hideo Hosono
Materials and Structures Laboratory, Mail Box R3-1, Tokyo Institute of Technology, 4259 Nagatsuta, Midori-ku, Yokohama, 226-8503, Japan

Structural, electronic, and optical properties of amorphous and transparent zinc tin oxide films deposited on glass substrates by pulsed laser deposition (PLD) were examined for two chemical compositions of Zn:Sn=1:1 and 2:1 as a function of oxygen partial pressure (P_{O_2}) used for the film deposition and annealing temperature. Different from a previous report on sputter-deposited films [Chiang *et al.*, Appl. Phys. Lett. **86**, 013503 (2005)], the PLD-deposited films crystallized at a lower temperature <450 °C to give crystalline ZnO and SnO_2 phases. The optical band gaps (Tauc gaps) were 2.80−2.85 eV and almost independent of oxygen P_{O_2}, which are smaller than those of the corresponding crystals (3.35−3.89 eV). Films deposited at low P_{O_2} showed significant subgap absorptions, which were reduced by postthermal annealing. Hall mobility showed steep increases when carrier concentration exceeded threshold values and the threshold value depended on the film chemical composition. The films deposited at low $P_{O_2}<2$ Pa had low carrier concentrations. It is thought that the low P_{O_2} produced high-density oxygen deficiencies and generated electrons, but these electrons were trapped in localized states, which would be observed as the subgap absorptions. Similar effects were observed for 600 °C crystallized films and their resistivities were increased by formation of subgap states due to the reducing high-temperature condition. High carrier concentrations and large mobilities were obtained in an intermediate P_{O_2} region for the as-deposited films. © 2008 American Vacuum Society. [DOI: 10.1116/1.2839860]

I. INTRODUCTION

Demands for visibly transparent and electrically conductive materials are rapidly growing in technological applications in optoelectronic devices such as solar cells, liquid crystal displays, energy efficient windows, and "invisible electronic circuits." A few crystalline materials such as tin doped indium oxide (ITO), aluminum doped zinc oxide (ZnO:Al), and antimony doped tin oxide (SnO_2:Sb) are presently being used for such applications. Zinc tin oxide films have the advantages of both ZnO (higher transparency and more stability in activated hydrogen environments than ITO and SnO_2) and SnO_2 (high stability in acidic and basic solutions and in oxidizing environments at higher temperatures).[1–6] Zinc tin oxide films have been grown by radio frequency and direct current magnetron sputtering, filtered vacuum arc deposition, etc., and most of these works have been devoted to understanding the optical and electrical properties of polycrystalline films fabricated by either substrate heating or high temperature postdeposition annealing.[7–11]

Amorphous transparent conductors are very attractive because they need a low processing temperature and have an ability to grow on plastic substrates in order to form high-quality films applicable to practical devices. Since the mobility of conduction electrons is proportional to the width of the conduction bands and a narrow band tends to localize carriers, a large overlap between relevant orbitals is required to achieve a large mobility degenerate conduction in amorphous semiconductors. In addition, the magnitude of the orbital overlap needs to be insensitive to the structural randomness, which is intrinsic to the amorphous state, to reduce the formation of shallow localized states (often referred to as tail states). Metal oxides composed of heavy metal cations (HMCs) with an electronic configuration $(n-1)d^{10}ns^0$ (with $n \geq 4$) satisfy these requirements. A large band gap in oxides is attained by the low energy of oxygen $2p$ orbitals, which constitute the valence band maximum region. The bottom part of the conduction band in these oxides is primarily composed of ns orbitals of HMCs.[12,13]

Amorphous silicon (*a*-Si) channel thin film transistors (TFTs), which are widely used as switching devices in active matrix liquid crystal displays (AMLCDs), suffer from their low field effect mobility (~ 1.0 cm^2 V^{-1} s^{-1}), photo/bias induced instability, and generation of photo-excited carriers because of the small band gap (~ 1.7 eV) (if no shadow mask is used in the devices). TFTs using transparent oxide semiconductors (TOSs) as the channel layer have several merits compared with the conventional Si-TFTs when applied to flat panel displays. These include the insensitivity of device performance to visible light illumination and efficient use of backlight in LCDs or emitted light in organic light-emitting diodes (OLEDs).[14] In addition, oxide TFTs have potential advantages over the covalent semiconductor-based TFTs in terms of their high voltage, temperature, and radiation tolerances.

Amorphous transparent semiconductor based TFTs have recently been investigated by several research groups. This includes the use of *a*-GaN,[15] *a*-IGZO,[16,17] *a*-ZTO,[18,19] *a*-IZO,[20–22] and *a*-Cd-In-Sb-O (Ref. 23) as active channel layers.[24–27] Devices fabricated from them have relatively high mobilities despite their amorphous nature. In TFTs fabricated by Chiang *et al.*, channel layers are sputter deposited from targets having the Zn:Sn ratios 1:1 and 2:1. Substrates were heated at 175 °C and devices were furnace annealed up to 600 °C.[18] Görrn *et al.* have studied the stability of transparent zinc tin oxide (ZTO) TFTs where the channel layer was deposited by pulsed laser deposition (PLD) of ZTO with Zn:Sn atomic ratios varying from 1:1 to 2:1.[19] Although TFT characteristics have recently been reported for amorphous ZTO, detailed study on their properties in relation to deposition condition, chemical composition, and postannealing has not been reported from the viewpoint of semiconductor materials. In this paper we focus on the preparation and characterization of room temperature (RT) deposited ZTO thin films prepared by PLD from the viewpoint of TFT channel materials.

II. EXPERIMENTAL DETAILS

Films were deposited at RT by PLD from ceramic targets of ZTO with a KrF excimer laser (248 nm wavelength, 10 Hz repetition frequency). Polycrystalline ceramics targets of $ZnO \cdot SnO_2$ (Zn:Sn=1:1 and 2:1) were prepared from a mixture of ZnO (99.999% pure) and SnO_2 (99.999% pure) powders. The mixed powders were initially calcinated at 1000 °C for 4 h and then hydrostatically pressed at a pressure of 1000 kg cm^{-2} to form a pellet of 1 cm diameter. The pellets were then sintered at 1450 °C for 6 h. The Zn:Sn =2:1 target forms a single phase compound of Zn_2SnO_4, and the other composition target leads to a mixture of ZnO, SnO_2, and Zn_2SnO_4, which were confirmed by x-ray diffraction (XRD) measurements. Laser ablation was carried out at a laser energy density of ~ 35 mJ cm^{-2} pulse^{-1}. Films were deposited on glass substrates placed at a distance of 30 mm from the target. The depositions were carried out for 30 min by varying oxygen pressure (P_{O_2}) from 0 to 9 Pa. The resulting film thicknesses varied from 110 to 200 nm. To study the
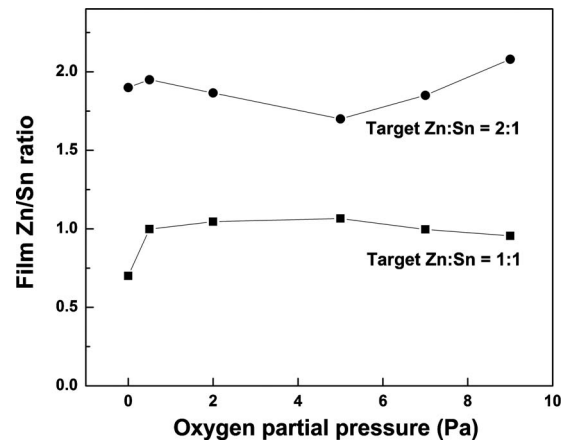

FIG. 1. Zn/Sn compositional variations with respect to oxygen partial pressure for the films deposited using different PLD targets with the Zn:Sn ratios of 1:1 and 2:1.

effects of postdeposition annealing on film properties, some films were annealed at temperatures up to 800 °C in air.

Structural characterization of the films was carried out by glancing incident x-ray diffraction analyses (GXRD, using RIGAKU RINT-2000 with Cu $K\alpha$ radiation) at the incident angle of 0.5°. Surface roughnesses of the films were evaluated by atomic force microscopy (AFM). Energy dispersive x-ray spectroscopy (EDX) was used for compositional analyses, and a UV-VIS-NIR spectrophotometer (Hitachi U-4000) was used for optical characterization. Resistivity, carrier concentration, and Hall mobility were obtained by Hall effect measurements using the van der Pauw configuration.

III. RESULTS AND DISCUSSION

A. Film chemical composition

Figure 1 shows the compositional variation in the films with P_{O_2}. It was confirmed that the Zn/Sn ratios of the sintered targets were the same as those of the corresponding starting compositions. Film composition shows some variation with P_{O_2}, but is more or less the same as that of the PLD target, indicating that the PLD process can reproduce the chemical composition of the target in the films if an appropriate deposition condition is chosen.

B. Film structure

Figure 2 shows GXRD patterns of the films deposited using PLD targets with the Zn:Sn ratios of 1:1 and 2:1 as a function of postannealing temperature. It shows that the deposited films are amorphous, but 450 °C annealing crystallizes the films partially to give crystalline phases of the simple oxides, ZnO and SnO_2. The halos around $2\theta = 33°$ indicate that some or a large portion of the amorphous phases still remain. This result should be compared with the results by sputtering in Refs. 18 and 9 in which the former reports no crystallization up to 600 °C and the latter reports the crystallization temperature is ~ 600 °C. This discrepancy would be attributed to the different growth kinetics of the
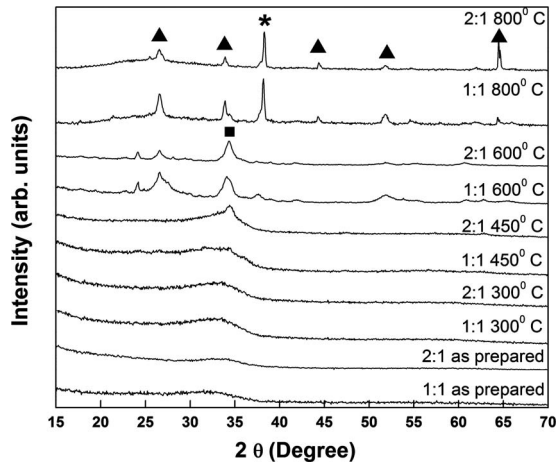
FIG. 2. GXRD patterns of the films deposited from targets having Zn:Sn compositions 1:1 and 2:1 as a function of annealing temperature. Zn:Sn ratio and annealing temperature are shown above the corresponding GXRD patterns. The triangles denote SnO$_2$, the square ZnO, and the asterisk ZnSnO$_3$. Resulting films deposited at RT and annealed up to 300 °C are amorphous, while crystallizing at 450 °C. SnO$_2$ and ZnSnO$_3$ phases are prominent in the crystallized films.

films between PLD and sputtering, where in general deposition precursors have larger kinetic energies for PLD owing to the excitation by high energy laser pulses and few collisions of the deposition precursors with gaseous molecules due to a lower P_{O_2} deposition condition. That is, it is speculated that higher energy precursors in PLD deposition form a more relaxed amorphous structure that is more easily crystallized. Further higher temperature annealing at 600–800 °C eliminates the remaining amorphous phases, producing a new crystalline phase ZnSnO$_3$ as a consequence of solid state reactions between the ZnO and SnO$_2$ phases segregated at 450–600 °C and the remaining amorphous ZTO film.[28,29]

Figure 3 shows the root-mean-squares (rms) surface roughness of the as-deposited films measured by AFM as a function of the chemical composition and P_{O_2}. It shows that the surface roughness depends on both the chemical compo-
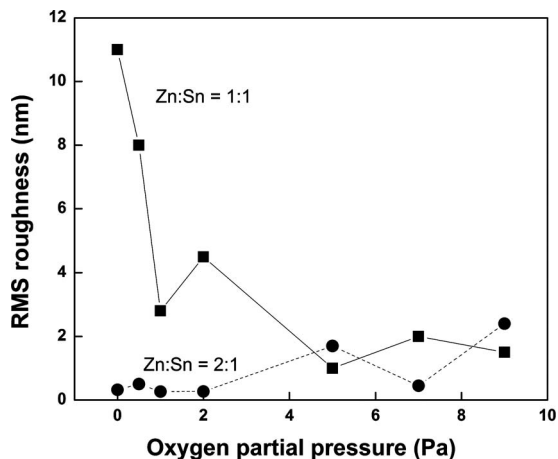

FIG. 3. Dependence of surface roughness on oxygen partial pressure for the films deposited from targets having Zn:Sn compositions 1:1 and 2:1.
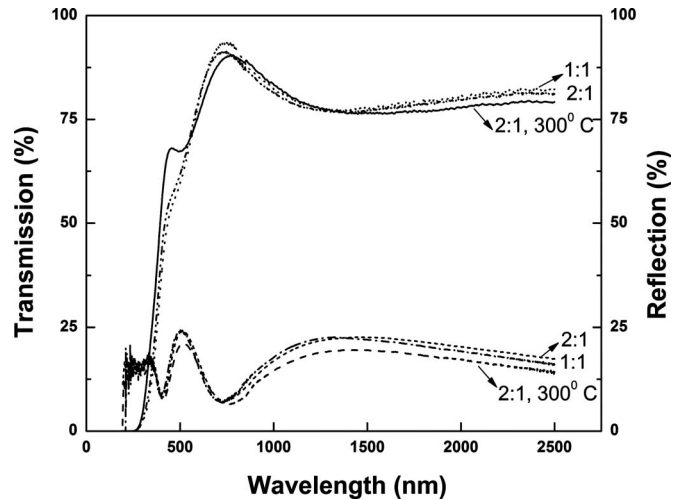
FIG. 4. Optical transmission and reflection spectra of the ZTO films prepared at P_{O_2}=0.5 Pa from targets having Zn:Sn compositions 1:1 and 2:1. The films are highly transparent across the visible region.

sition and P_{O_2} and ranges up to 11 nm. The films with the Zn:Sn composition 1:1 have larger roughness compared to the 2:1 composition films, and its roughness decreases with the increase of P_{O_2}. The films deposited from the Zn:Sn =2:1 target have atomically flat surfaces with surface roughness less than 0.3 nm at low P_{O_2}≤2 Pa. The surface flatness of an active layer is an important parameter because carrier transport in TFT channels is significantly affected by the carrier scattering due to roughness at the channel-gate insulator interface.[30]

C. Optical properties

Figure 4 shows transmittance/reflectance spectra of the ZTO films deposited at a P_{O_2} of 0.5 Pa. It shows that the ZTO films have average transmittances >85% in the visible region and significant difference is not observed for the films having different chemical compositions.

The optical absorption coefficient α of semiconductors generally follows a relationship of the form

$$\alpha h\nu = (\mathrm{cont})(h\nu - E_g^{\mathrm{opt}})^r,$$

where $h\nu$ denotes the photon energy, E_g^{opt} is the optical band gap, and r is a constant depending on the model. The E_g^{opt} value is then obtained by linearly extrapolating the plot of $(\alpha h\nu)^{1/r}$ vs $h\nu$ and finding the intersection with the abscissa. Tauc *et al.* showed that $r=2$ holds in amorphous semiconductors assuming a parabolic band and a constant transition moments;[31] this behavior is indeed found for many amorphous semiconductors.[32] The optical data in Fig. 4 were analyzed with $r=2$ (Tauc plot) [Figs. 5(a) and 5(b)], which derived E_g^{opt} values 2.37–2.86 eV varying with P_{O_2} as summarized in Fig. 5(c). There is some uncertainty in the estimation of E_g^{opt} at low P_{O_2} due to the presence of subgap states. The E_g^{opt} value is insensitive to P_{O_2} at P_{O_2}≥2 Pa. It should be noticed that the fundamental band gap is an intrinsic property of a material: however, the exceptionally small
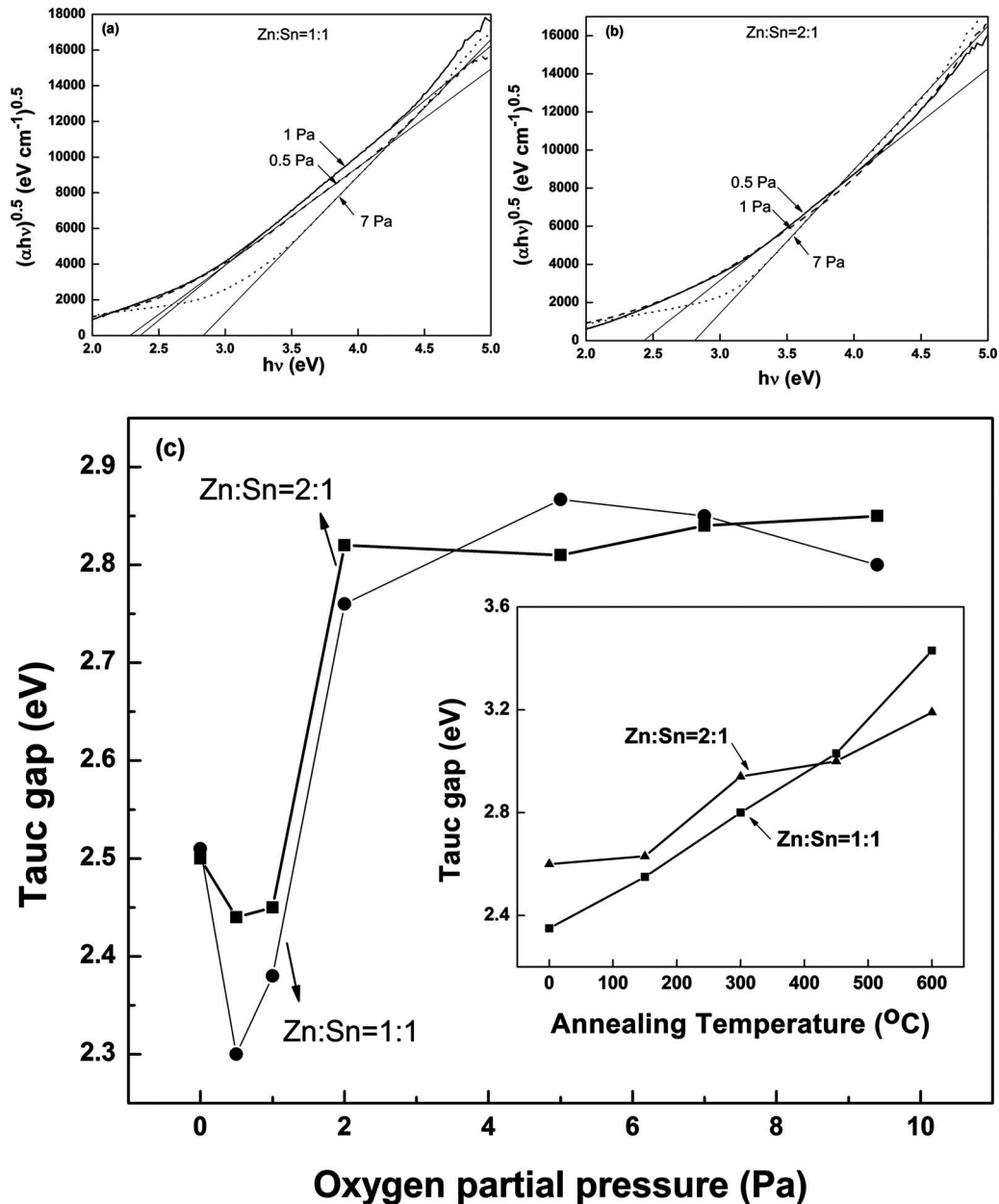
FIG. 5. (a) Tauc plots for the films prepared from the Zn:Sn=1:1 target at different P_{O_2}. (b) Tauc plots for the films prepared from the Zn:Sn=2:1 target at different P_{O_2}. (c) Dependence of Tauc gap of the *a*-ZTO films on P_{O_2}. Inset shows the effect of annealing on Tauc gap of the films prepared at P_{O_2} =0.5 Pa.

E_g^{opt} values are obtained for the low P_{O_2} films, because strong subgap absorption bands appear beneath the fundamental band gap and superimpose with the fundamental band absorption as will be observed in Fig. 6. These results should also be compared with previously reported results. As summarized in the Introduction of Ref. 18 and reported in Ref. 9, the Tauc gaps of ZTO films are 3.35–3.89 eV. But these films are crystallized, and therefore they should not be compared with the present data for amorphous ZTO. It indicates that the fundamental optical gaps of ZTO films are reduced to 2.8–2.86 eV by amorphization.

Figure 6 is log α–$h\nu$ plots that show subgap absorption more clearly. It is observed that the as-deposited films have

orders of magnitude larger absorption below the fundamental band gap of ~2.8 eV when deposited at low $P_{O_2} \leq 2$ Pa [Figs. 6(a) and 6(b)], which causes the exceptionally small apparent E_g^{opt} values obtained above. At higher P_{O_2}, even though some subgap absorptions remain, they are more distinguishable from the fundamental band absorptions and give larger Tauc gaps>2.8 eV. It is also found that thermal annealing at ≥ 150 °C reduces the strong subgap absorptions observed in the low P_{O_2} films [Fig. 6(c)], and 300 °C annealing increases the Tauc gaps to >2.8 eV as summarized in the inset to Fig. 5. The large increase in the subgap absorption for the 600 °C annealed films would be attributed to
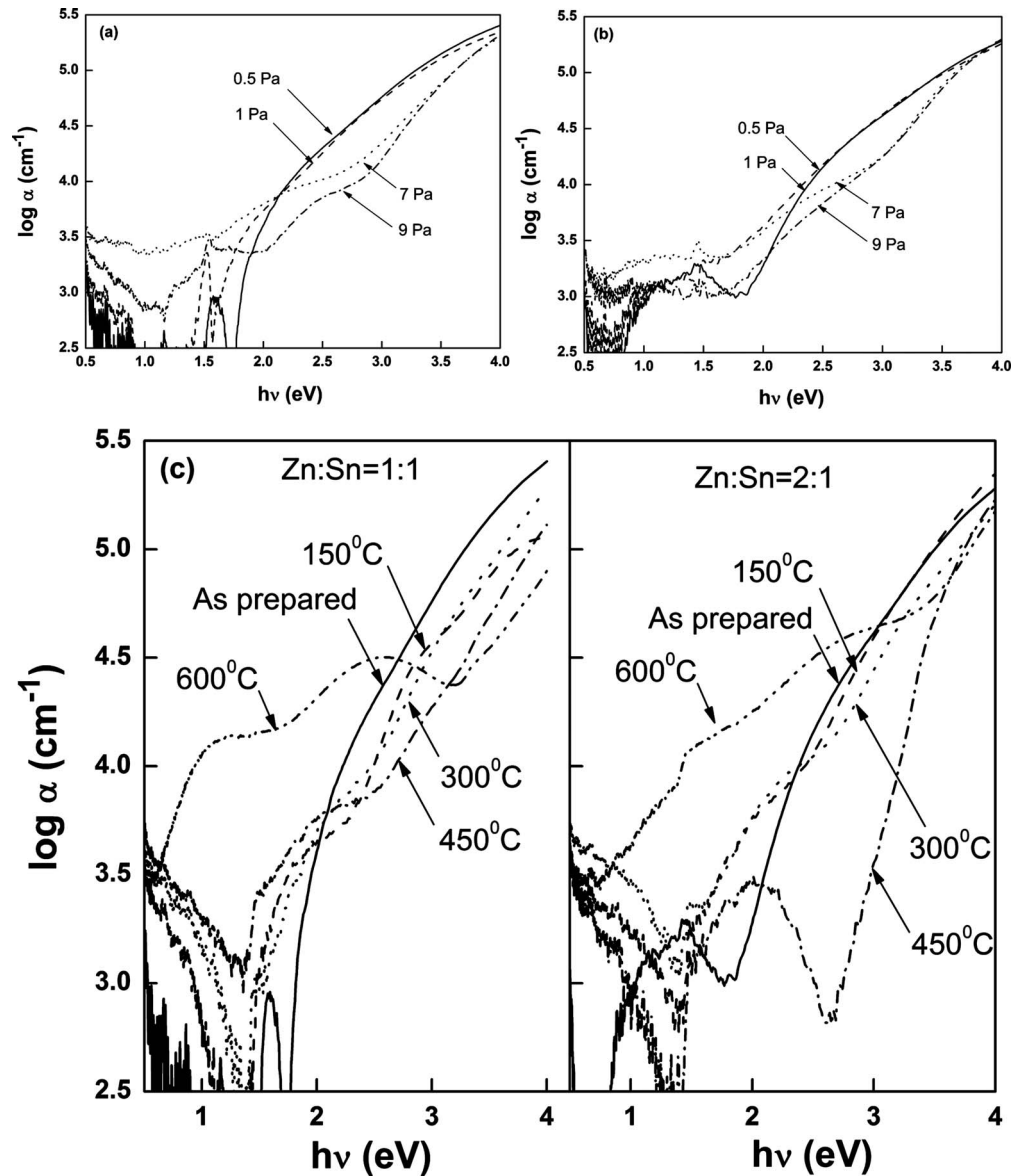
FIG. 6. log $\alpha-h\nu$ plots for ZTO films. (a) As-prepared films deposited from the target of the Zn:Sn composition 1:1. (b) As-prepared films deposited from the target of the Zn:Sn composition 2:1. (c) Annealed films (deposited at P_{O_2}=0.5 Pa) as a function of annealing temperature.

a strong reduction condition of the high temperature and formation of many oxygen deficiencies.

D. Electrical properties

Electrical properties of the as-deposited *a*-ZTO films are summarized in Fig. 7. Previous papers on a disordered crystalline oxide semiconductor[33] and amorphous oxide semiconductors[16,30,34] indicate that carrier concentration should exceed a threshold value to obtain a large mobility needed for semiconductor devices using active layers with structural randomness. Similar to them, Hall mobilities comparable to or greater than 10 cm^2 V^{-1} s^{-1} are obtained in the *a*-ZTO films when the carrier concentrations exceed $\sim10^{16}$ cm^{-3} for the Zn:Sn=2:1 films and $\sim10^{18}$ cm^{-3} for the Zn:Sn=1:1 films.

Figure 8(a) shows the controllability of the carrier concentration for the as-deposited ZTO films. Carrier concentra-
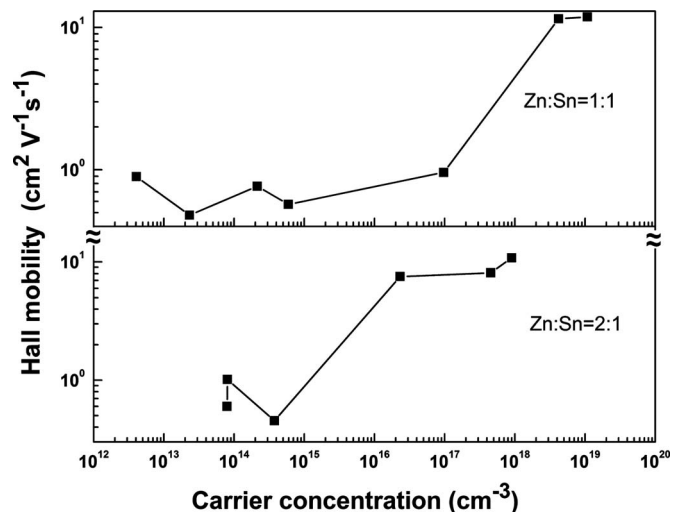

FIG. 7. Relationship between Hall mobility and carrier concentration in the as-deposited *a*-ZTO films.
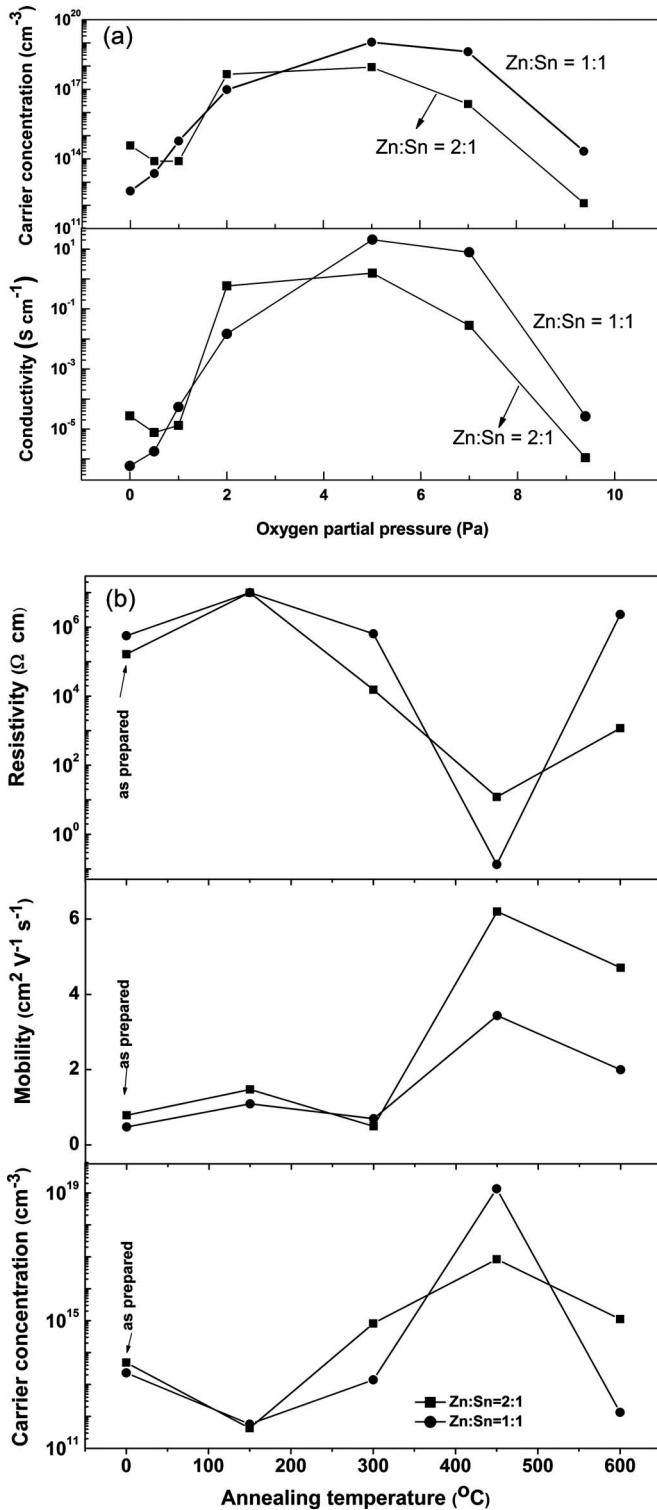
FIG. 8. Dependences of carrier transport properties on (a) oxygen partial pressure for the as-deposited films and on (b) postannealing temperature for the films deposited at $P_{O_2}=0.5$ Pa.

contribute to form donor states. However, the low carrier concentrations at low P_{O_2} are not common in PLD deposited transparent conducting oxides. It would be explained for the ZTO films by the large subgap states below 3 eV observed in Fig. 6. Effects of postthermal annealing on the electrical properties of the films prepared at 0.5 Pa are shown in Fig. 8(b). Figure 6(c) showed that the postthermal annealing decreases the total subgap states. Up to 450 °C, there is a reduction of total subgap states that enhances the carrier concentration and hence the mobility. In the case of the 600 °C annealing, it again produces a large number of subgap states, although almost all the films become polycrystalline phases as observed in Fig. 2. It suggests that the contribution of reducing atmosphere at the high temperature increases defects (e.g., oxygen deficiencies) and localized states, which increases the film resistivity.

IV. CONCLUSION

The structural, electrical, and optical properties of amorphous zinc tin oxide films deposited by pulsed laser deposition were investigated for two Zn/Sn compositions as a function of oxygen partial pressure (P_{O_2}) and annealing temperature. The effects of postdeposition annealing on the optical and electrical properties of ZTO films were also examined. It was found that optical absorption spectra showed strong subgap absorptions if the films were deposited at low $P_{O_2}<2$ Pa. Tauc gaps of the ZTO films were increased to 2.80–2.85 eV by high P_{O_2} deposition or postthermal annealing, which resulted from the reduction of the subgap states. The carrier concentration-P_{O_2} relations showed broad peaks, which is explained by the existence of the electron traps in the subgap states for the low P_{O_2} films and by the reduction of the oxygen deficiencies for the high P_{O_2} films. The high electron concentration films showed large Hall mobilities greater than 10 cm²/V s.

[1] S. Major, S. Kumar, M. Bhatnanger, and K. L. Chopra, Appl. Phys. Lett. **49**, 394 (1986).
[2] T. Minami, H. Sato, H. Nanto, and S. Takata, Thin Solid Films **176**, 277 (1989).
[3] Z. C. Jin, I. Hamberg, and C. G. Granqvist, J. Appl. Phys. **64**, 5117 (1988).
[4] J. Hu and R. G. Gordon, J. Appl. Phys. **71**, 880 (1992).
[5] R. J. Cava, J. M. Phillips, J. Kwo, G. A. Thomas, R. B. van Dover, S. A. Carter, J. Krajewski, W. F. Peck, Jr., J. H. Marshall, and D. H. Rapkine, Appl. Phys. Lett. **64**, 2071 (1994).
[6] K. L. Chopra, S. Major, and D. K. Pandya, Thin Solid Films **102**, 1 (1983).
[7] T. Minami, S. Takata, H. Sato, and H. Sonohara, J. Vac. Sci. Technol. A **13**, 1095 (1995).

tion can be controlled from $\sim 10^{12}$ to 10^{19} cm^{-3} by varying P_{O_2} from 0 to 5 Pa. The large carrier concentrations and mobilities are obtained for the P_{O_2} range of 2–7 Pa. The decrease of carrier concentration at higher P_{O_2} is due to the suppression of the formation of oxygen deficiencies that may

[8]D. L. Young, D. L. Williamson, and T. J. Coutts, J. Appl. Phys. **91**, 1464 (2002).

[9]D. L. Young, H. Moutinho, Y. Yan, and T. J. Coutts, J. Appl. Phys. **92**, 310 (2002).

[10]T. Moriga, Y. Hayashi, K. Kondo, Y. Nishimura, K. Murai, I. Nakabayashi, H. Fukumoto, and K. Tominaga, J. Vac. Sci. Technol. A **22**, 1705 (2004).

[11]E. Cetinorgu, S. Goldsmith, and R. L. Boxman, Thin Solid Films **515**, 880 (2006).

[12]H. Hosono, N. Kikuchi, N. Ueda, and H. Kawazoe, J. Non-Cryst. Solids **198–200**, 165 (1996).

[13]H. Hosono, J. Non-Cryst. Solids **352**, 851 (2006).

[14]P. Görrn, M. Sander, J. Meyer, M. Kroger, E. Becker, H. H. Johaness, W. Kowalsky, and T. Riedl, Adv. Mater. **18**, 738 (2006).

[15]S. Kobayashi, S. Nonomura, T. Ohmori, K. Abe, S. Hirata, T. Uno, T. Gotoh, S. Nitta, and S. Kobayashi, Appl. Surf. Sci. **113–114**, 480 (1997).

[16]K. Nomura, H. Ohta, A. Takagi, T. Kamiya, M. Hirano, and H. Hosono, Nature (London) **432**, 488 (2004).

[17]H. Yabuta, M. Sano, K. Abe, T. Aiba, T. Den, H. Kumomi, K. Nomura, T. Kamiya, and H. Hosono, Appl. Phys. Lett. **89**, 112123 (2006).

[18]H. Q. Chiang, J. F. Wager, R. L. Hoffman, J. Jeong, and D. A. Keszler, Appl. Phys. Lett. **86**, 013503 (2005).

[19]P. Görrn, P. Holzer, T. Riedl, W. Kowalsky, J. Wang, T. Weimann, P. Hinze, and S. Kipp, Appl. Phys. Lett. **90**, 063502 (2007).

[20]J. I. Song, J. S. Park, H. Kim, Y. W. Heo, J. H. Lee, J. J. Kim, G. M. Kim, and B. D. Choi, Appl. Phys. Lett. **90**, 022106 (2007).

[21]N. L. Dehuff, E. S. Kettenring, D. Hong, H. Q. Chiang, J. F. Wager, R. L. Hoffman, C. H. Park, and D. A. Keszler, J. Appl. Phys. **97**, 064505 (2005).

[22]P. Barquinha, P. Pimentel, A. Marques, L. Pereira, R. Martins, and E. Fortunato, J. Non-Cryst. Solids **352**, 1756 (2006).

[23]H. Tetsuka, Y. J. Shan, K. Tezuka, and H. Imoto, Vacuum **80**, 1038 (2006).

[24]R. Martins, P. Barquinha, I. Ferreira, L. Pereira, G. Goncalves, and E. Fortunato, J. Appl. Phys. **101**, 044505 (2007).

[25]R. Martins, P. Barquinha, L. Pereira, I. Ferreira, and E. Fortunato, Appl. Phys. A **89**, 37 (2007).

[26]M. S. Grover, P. A. Hersh, H. Q. Chiang, E. S. Kettenring, J. F. Wager, and D. A. Keszler, J. Phys. D **40**, 1335 (2007).

[27]M. Kim, J. H. Jeong, H. J. Lee, T. K. Ahn, H. S. Shin, J. S. Park, J. K. Jeong, Y. G. Mo, and H. D. Kim, Appl. Phys. Lett. **90**, 212114 (2007).

[28]Joint Committee on Powder Diffraction Standards, _Powder Diffraction File Card No. 21–1250_ (ASTM, Philadelphia, PA, 1967).

[29]D. Kovacheva and K. Petrov, Solid State Ionics **109**, 327 (1998).

[30]K. Nomura, A. Takagi, T. Kamiya, H. Ohta, M. Hirano, and H. Hosono, Jpn. J. Appl. Phys., Part 1 **45**, 4303 (2006).

[31]J. Tauc, R. Grigorovici, and A. Vancu, Phys. Status Solidi B **15**, 627 (1966).

[32]J. Tauc, _Amorphous and Liquid Semiconductors_ (Plenum, New York, 1979).

[33]K. Nomura, T. Kamiya, H. Ohta, K. Ueda, M. Hirano, and H. Hosono, Appl. Phys. Lett. **85**, 1993 (2004).

[34]A. Takagi, K. Nomura, H. Ohta, H. Yanagi, T. Kamiya, M. Hirano, and H. Hosono, Thin Solid Films **486**, 38 (2005).